

論 文

Graphite Spheroidization in Cast Iron by Addition of Misch Metal Hydrides

Kwan-Hyu Kim,* Doh-Jae Lee*, Dap-Chun Choi* and Choong-Nyeun Park*

鑄鐵의 黑鉛구상화에 미치는 Misch Metal Hydride의 添加效果

김관휴*, 이도재*, 최답천*, 박충년*

Abstract

3.9%C-2.0%Si-Fe 조성의 壓粉體를 1350℃, Ar가스 분위기에서 50분간 용해한 용탕에 市販 misch metal과 misch metal hydride 인 MmH와 MmH₂를 각각 여러비율로 添加한후 徐冷및 急冷한 시편의 黑鉛形狀의 변화로부터 misch metal hydride의 球狀化能과 黑鉛球狀化 機構로서의 氣泡說의 타당성을 고찰한 결과 다음과 같은 결론을 얻었다.

1) Misch metal은 0.5% 이상, 그리고 misch metal hydride는 0.25% 이상 첨가한 때 球狀黑鉛과 CV黑鉛이 나타났으며, misch metal hydride를 첨가한 때가 misch metal에 비하여 黑鉛粒數가 더 많았다. 이와같이 misch metal hydride의 첨가량이 misch metal에 비하여 적었음에도 黑鉛粒數가 더 많은 것을 보면 Mm으로부터 방출되는 多數의 水素氣泡가 球狀黑鉛의 精출장소로 되는 것으로 해석되기 때문에 氣泡說이 타당하다고 생각된다.

2) Misch metal 과 misch metal hydride의 添加量이 1.0%로 증가되면 두경우 모두 黑鉛粒數가 감소하였다. 이는 용탕중에 개재된 水素氣泡의 실수율차이에 의한 잔류 수소기포수의 증가율둔화와 添加量의 증가에 따른 잔류 misch metal량의 相對的 증가로 인한 다량의 잔류 misch metal이 응고과정에서 수소를 재흡수 용해하여 흑연입수를 결정하는 용탕중의 有效水素氣泡數를 감소시켰기 때문으로 생각된다.

1. Introduction.

It has been well known that cerium itself(1) or an addition of cerium to Mg-Fe-Si nodulizer(2) can produce spheroidal graphites or increases the nodule counts in cast iron. The role of cerium in spheroidal graphite cast iron has been reported to be a desulfurization and an inhibition of carbide decomposition(1,3)or a provider of hydrogen bubbles which can be nucleation sites of the spheroidal graphites(4,5).

The latter is based on the bubble theory for the spheroidization mechanism of graphite in cast iron. The bubble theory proposed by Chang et al.(4-10) states that if the bubbles such as H₂, CO or Mg vapor are somehow introduced into the melt, the graphites can precipitate on the bubble surfaces and grow into the center of bubbles by diffusion of carbon from the carbon supersaturated melt. When there is excess carbon in the melt over the completion of the centrifugal growth the graphites grow outward from the surface. This theory might be able to account for the presence of bubbles

전남대학교 공과대학 (*Dept. of Metallurgical Eng., College of Eng., Chonnam National University)

in the melt and the mechanisms for the growth, degeneration and fading of the spheroidal graphites. Suzuki et al.(11), however, have reported that hydrogen in the melt of cast iron inhibits the graphite spheroidization. Tsutsumi et al.(12) also have argued that the bubble theory can not explain the preferential growth of the spheroidal graphite which is dependent on the crystal direction. In addition, the other nucleation sites, for example, surfaces of the rare-earth sulfides (13), are not related with the bubbles.

In this study, we have attempted to recheck the bubble theory by applying *misch metal hydrides* as *nodulizers* because *misch metal hydrides* can provide a large proportion of the hydrogen bubbles and the number of the bubbles can be varied by variation of hydrogen content in the *misch metal* and the total amount of the *nodulizer* added.

2. Experimental.

The raw materials were electrolytic pure iron power, silicon powder and graphite powder for the cast iron, *misch metal* chips for the hydrides and *ferro-silicon* for the post inoculations. The chemical compositions of the raw materials are shown in Table 1 and Table 2. The *nodulizers* were *misch metal* (Mm), *misch metal monohydride*(MmH) and *misch metal dihydride* (MmH₂). The *misch metal hydrides* were prepared by hydrogenation of the *misch metal* chips with a given amount of hydrogen. The hydrogenation was carried out by a Sievert type volumetric apparatus(Fig.1). A charge of 40 grams which consisted of iron powder, 2.0% Si powder and 3.9% graphite powder was compacted, and melted in quartz crucible by using a vertical type SiC tube furnace at 1350°C (Fig.2). After holding at 1350°C for 50 minutes the given amount of *misch metal* or *misch metal hydride* *nodulizer* was added into the melt and then 0.3wt% of the *ferro-silicon* was added for the post inoculation. The temperature of the melt was stabilized 5 minutes after the post inoculation. Then, the quartz crucible was taken out from the furnace and put into the cooling mold which was made of an insulating block. During cooling a cooling curve was recorded and the maximum and minimum eutectic temperatures were

Table 1. Sieve and chemical analysis of iron, graphite and silicon powder.

	Sieve analysis		Chemical analysis	
	Tyler mesh	wt. %	Composition	wt. %
Fe powder	+ 100	0	C	0.02
	- 100 + 200	bal.	Si	0.006
	- 200 + 270	max. 20	P	0.005
	- 270 + 325	max. 9	S	0.005
	- 325	max. 8	Mn	0.01
			Fe	bal.
Graphite powder	+ 150	5	Fixed carbon	98
	- 150 + 250	5-20	Ash	1
	- 250	75-90	Volatile matter	1
Si powder	+ 325	1	Si	99
	- 325	99	Impurity	1

Table 2. Chemical composition of *mischmetal* and *ferro-silicon*.

	Chemical composition (wt. %)								
	C	Si	P	S	Fe	Ce	La	Nd	Other REM
Fe-Si	0.2	75-80	0.05	0.02	bal.	-	-	-	-
Misch-metal	-	-	-	-	-	48-50	32-34	13-14	bal.

determined from the curve. In order to see the changes of microstructures during the eutectic reaction, some samples were water-quenched from the temperatures which were 10°C higher prior to and 3°C high posterior to the the minimum eutectic temperature (Fig.3). The microstructures of the samples were investigated by using an optical microscope, and the nodule counts and the area of the spheroidal and CV graphites were measured by an image analyzer.

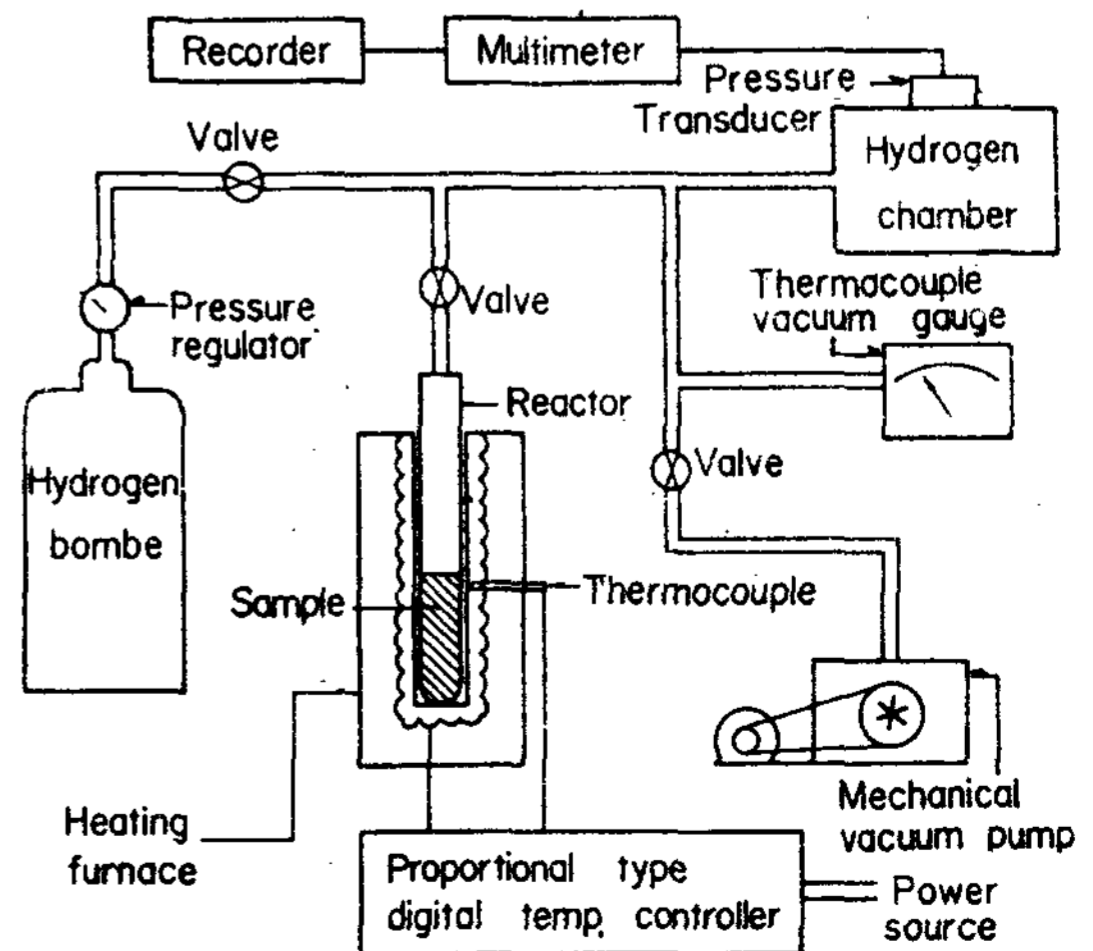


Fig. 1. Schematic diagram showing an apparatus for hydrogenating treatment.

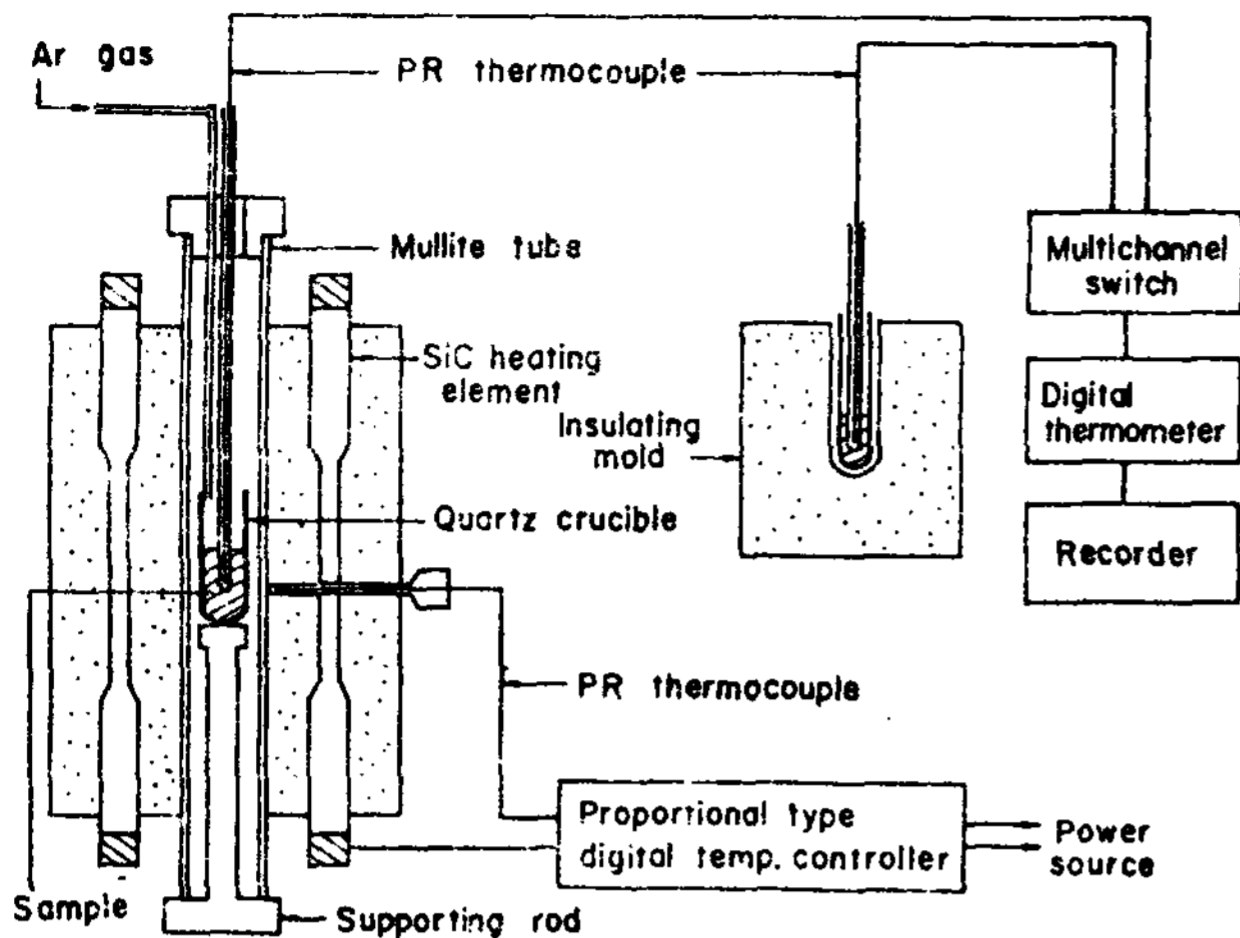


Fig. 2. Schematic diagram showing a furnace for melting and spheroidizing treatment.

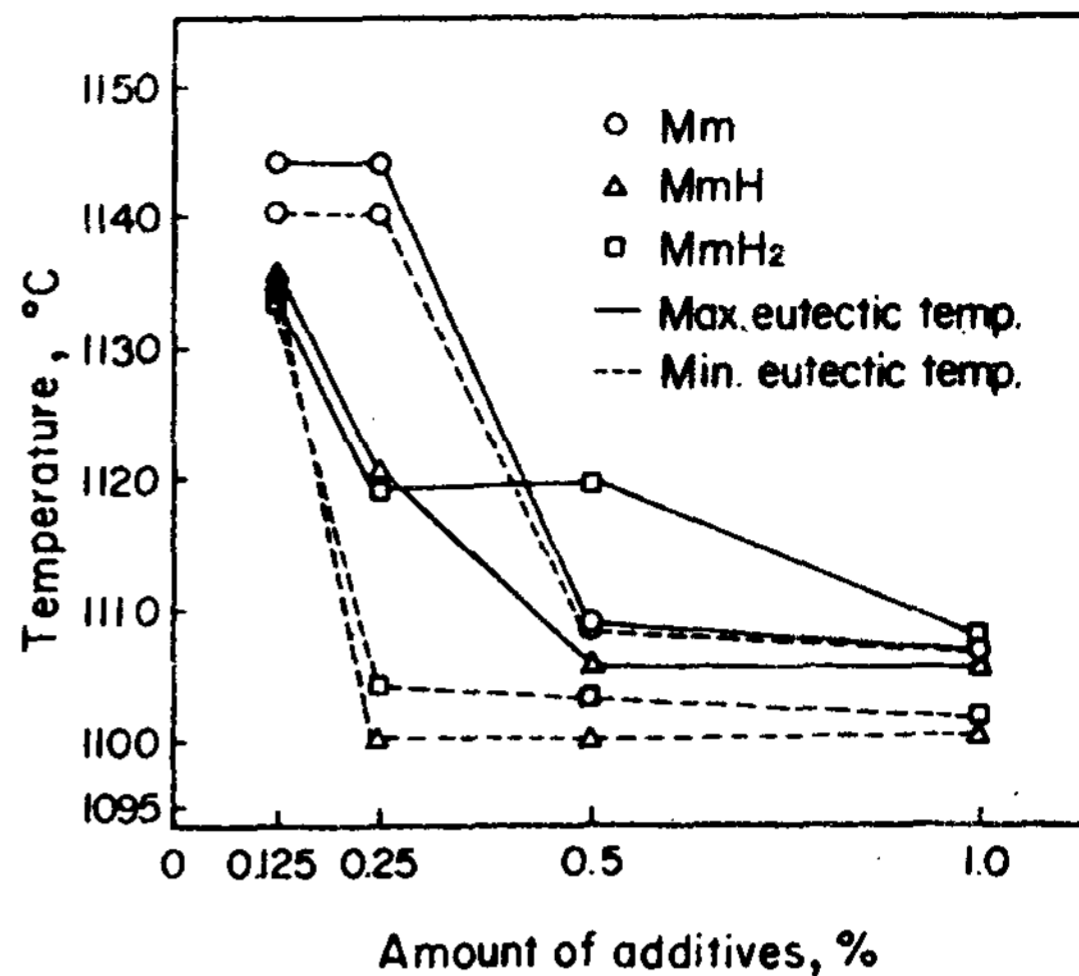


Fig. 4. Variation of the maximum and minimum eutectic temperatures with the amount of additives.

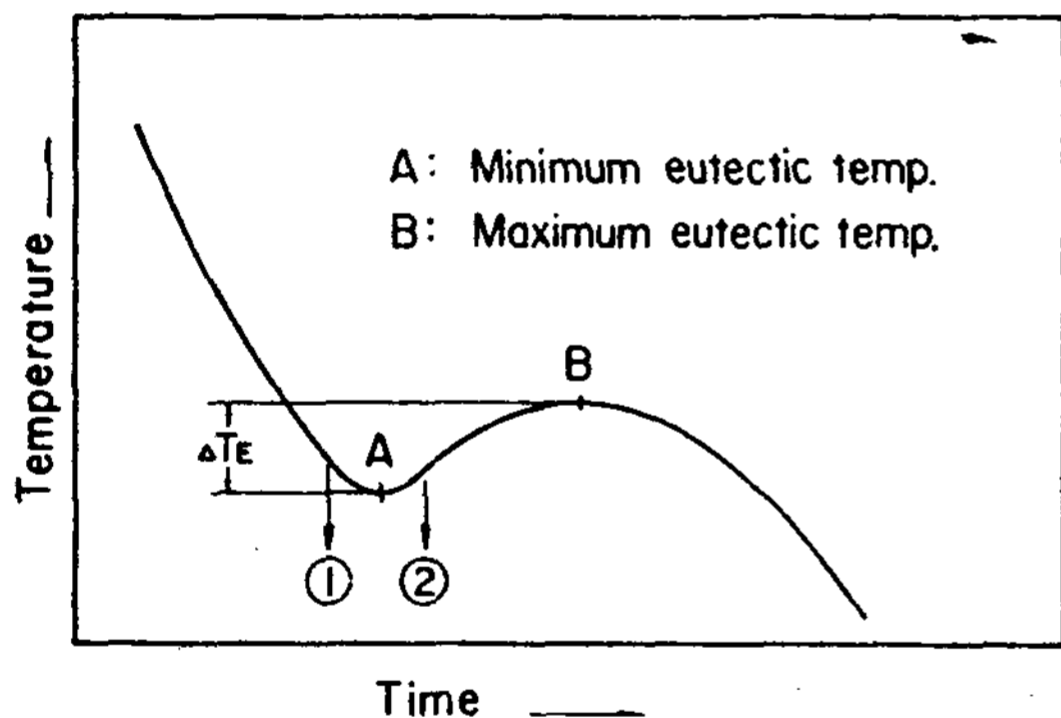


Fig. 3. Solidification cooling curve showing the maximum and minimum eutectic temperatures. The samples were water-quenched at points ① and ② respectively.

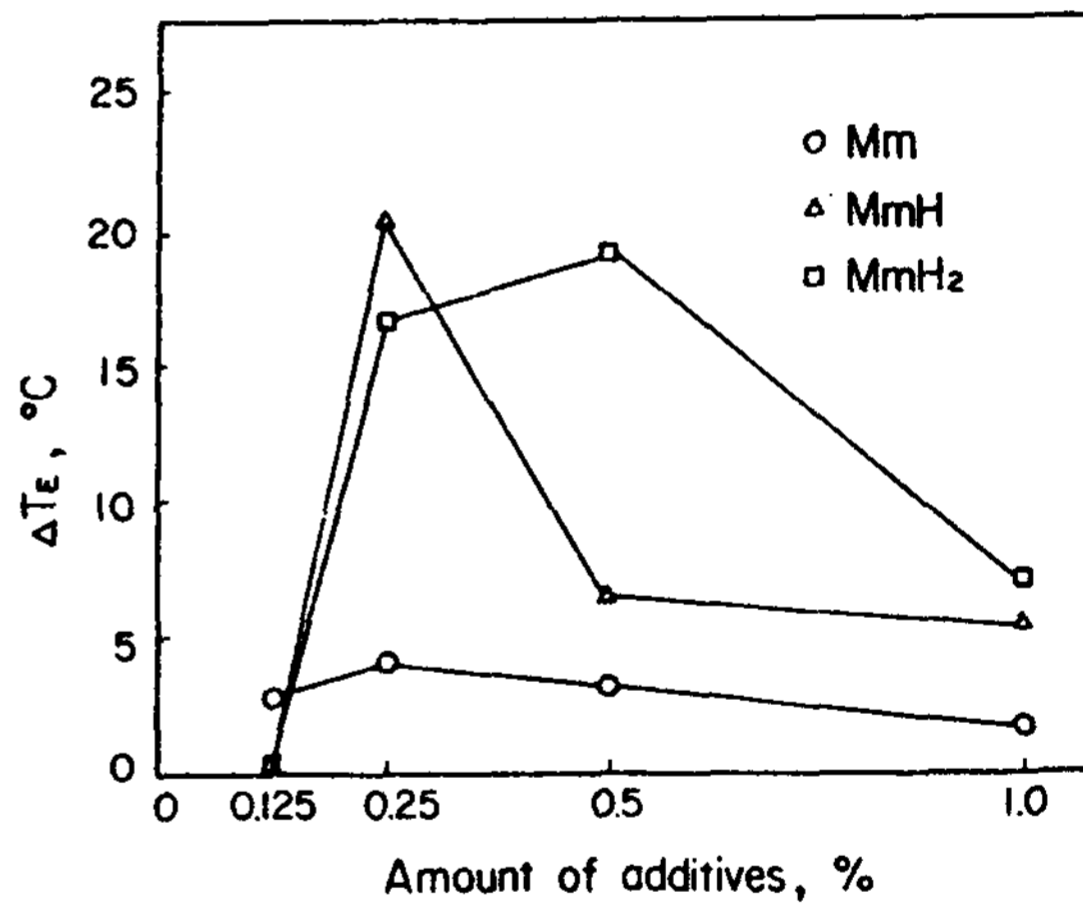


Fig. 5. Variation of ΔT_E with the amount of additives.

3. Results and Discussion.

The chemical compositions of the samples which were treated by 0.125, 0.25, 0.5 or 1.0wt % of Mm, MmH or MmH₂ are presented in Table 3. The maximum and minimum eutectic temperatures, $T_{E, max}$ and $T_{E, min}$, which were measured during slow cooling are shown in Fig. 4. It is seen from the Fig. 4 that the maximum and minimum eutectic temperatures decrease with increasing amount of the nodulizer addition and the extent of the decreases are dependent on the type of nodulizers.

The differences between them would appear clearly when the values of $\Delta T_E (= T_{E, max} - T_{E, min})$ were plotted with the amount of the additives (Fig. 5). Fig. 5 shows that ΔT_E values are large at intermediate amounts of the additives. The microstructures of each samples are shown in Photo. 1 and the graphite shapes of the samples are summarized in Table 4. As shown in Photo. 1 and Table 4, the graphite shapes of the samples can be classified into three types. These are, 1) Mixture of rosette graphite and undercooled graphite which were observed in each samples treated with the 0.125 %Mm, 0.25 %Mm, and 0.125 %MmH₂, 2) Mixture of spheroidal

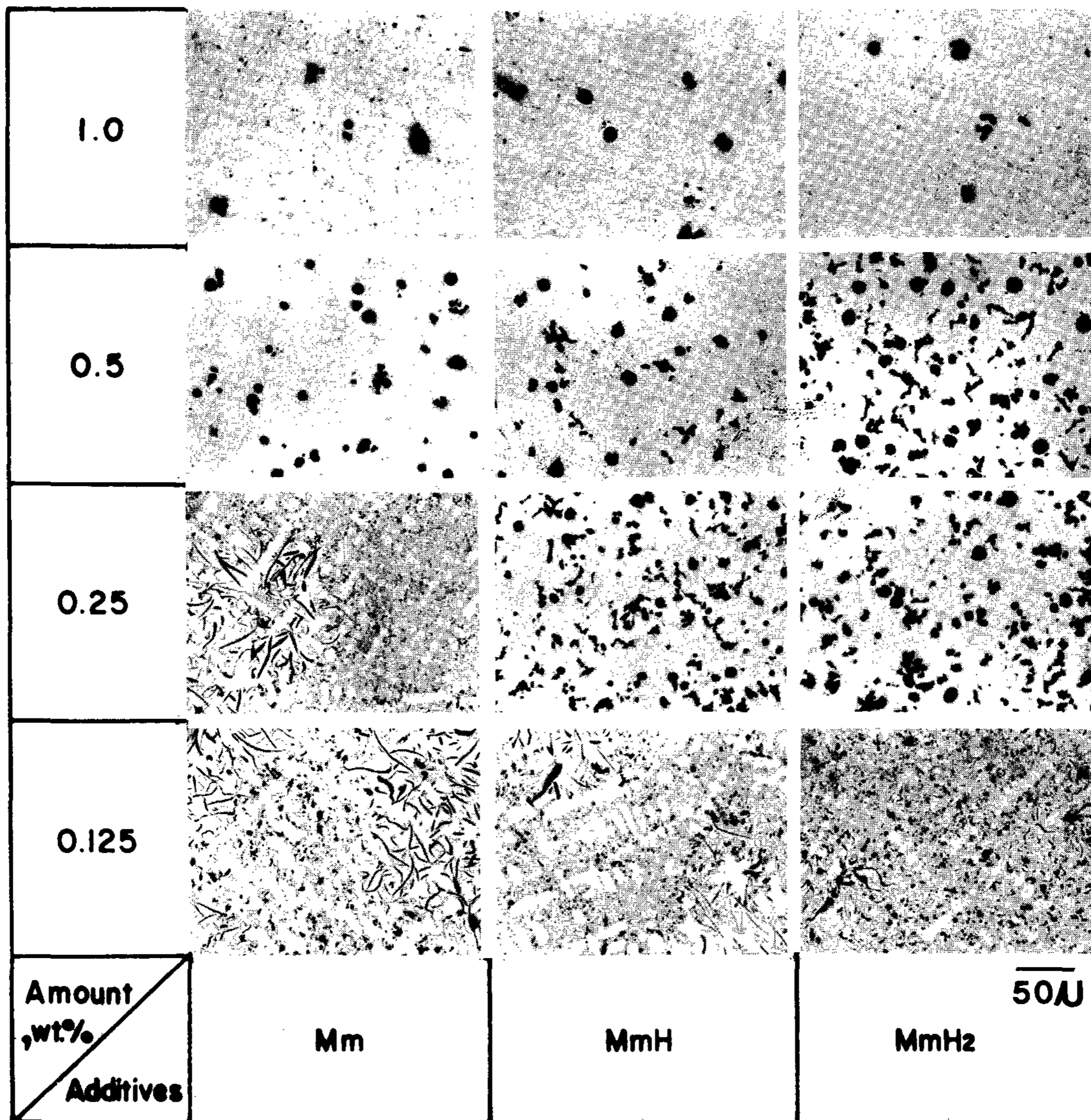


Photo. 1. Change of graphite shapes of the slowly cooled samples with the amount of mischmetal, MmH and MmH₂. As polished.

graphites and CV gtraphites with high counts which were observed in each sample treated with the 0.25 %MmH, 0.25 %MmH₂ and 0.5 %MmH₂, 3) Mixture of spheroidal graphites and imperfect spheroidal graphites with low counts which were observed in each sampke treated with 0.5 %Mm, 1.0 %Mm, 0.5 %MmH, 1.0 %MmH and 1.0 %MmH₂. The average nodule counts of the spheroidal and CV graphites were determined by the image analyzer and the results are shown in Fig.6. The microstructures of samples treated with the 0.25 %Mm,

0.5 %Mm, 0.25 %MmH and 0.5 %MmH, which were water-quenched at the early stage and intermediate stage of the eutectic reaction are shown in Photo.2. From the Photo.1 and the Table 4, the formation conditions and the growth characteristics of the three types of graphites can be clarified. The first type, mixture of the under-cooled gtraphite and the rosette graphite was formed when the maximum eutectic temperature was very high, i.e., 1134 to 1144°C and the eutectic super cooling was not so big. Thus the value of ΔT_E was very low and

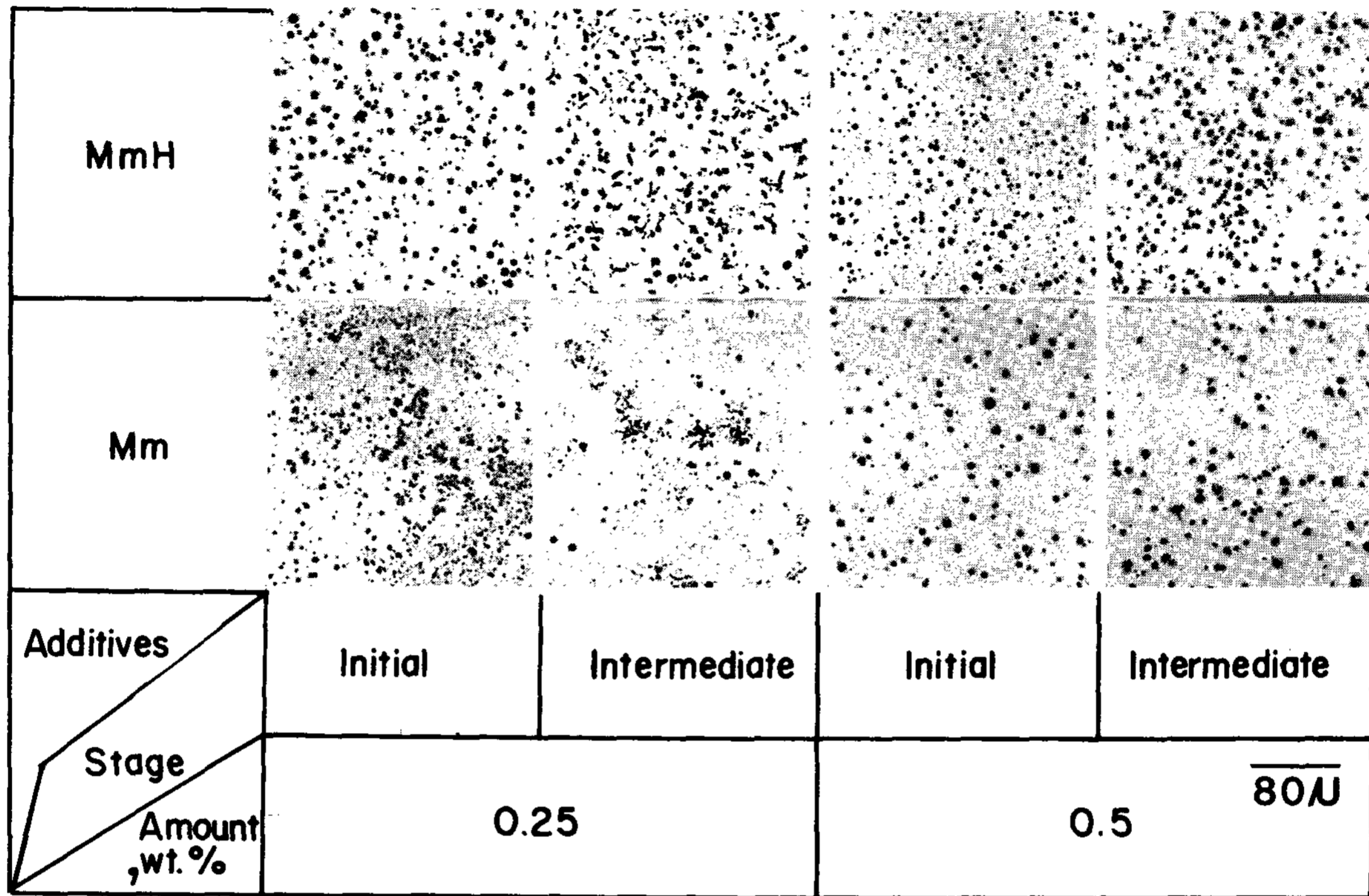


Photo. 2. Change of microstructures of the samples treated by mischmetal and MmH, and waterquenched during eutectic reaction. As polished.

Table 3. Chemical composition of samples.

Samples	Chemical composition (wt. %)				
	C	Si	S	Ce	Fe
Mm, 0.125 %	3.60	1.96	0.008	0.026	bal.
Mm, 0.25 %	3.61	1.99	0.007	0.034	bal.
Mm, 0.5 %	3.61	2.04	0.009	0.058	bal.
Mm, 1.0 %	3.62	2.05	0.008	0.130	bal.
MmH, 0.125 %	3.63	2.03	0.007	0.026	bal.
MmH, 0.25 %	3.62	1.95	0.007	0.028	bal.
MmH, 0.5 %	3.62	2.05	0.008	0.044	bal.
MmH, 1.0 %	3.60	2.01	0.006	0.076	bal.
MmH ₂ , 0.125 %	3.61	2.06	0.008	0.016	bal.
MmH ₂ , 0.25 %	3.64	2.11	0.007	0.028	bal.
MmH ₂ , 0.5 %	3.63	2.02	0.007	0.042	bal.
MmH ₂ , 1.0 %	3.62	2.05	0.006	0.084	bal.

less than 4 degrees. In this case, the hydrogen bubbles in the melt did not contribute to form spheroidal graphites. Instead, the rosette graphites nucleated in the undercooled graphites at the intermediate stage of eutectic reaction and grew, resulting in the final structure (Photo.2). The second type, mixture of the spheroidal graphite and the CV graphites, was obtained when the maximum and minimum eutectic temperatures were 1119 to 1121 °C and 1100 to 1101 °C respectively. The eutectic supercooling was big and the value of ΔT_E was very large upto 17 to 21 degrees. In this case, the nodule counts were very high, up to 180 to 194 n / mm². Many spheroidal graphites and imperfect spheroidal graphites appeared at the early stage of the eutectic reaction and developed into the mixed structure of the spheroidal and CV graphites at the intermediate and the final stages of the eutectic reaction. The third type, a mixture of the spheroidal and imperfect graphites, was produced when the maximum and minimum eutectic temperatures were very low i.e., 1105 to 1108 °C and 1098 to 1101 °C respectively. Although the eutectic supercooling was very

Table 4. Effect of additives and their amount on the graphite shapes.

Additives Amount, %	Mm	MmH	MmH ₂
0.125	IG + RG	IG + RG	IG + RG
0.25	IG + RG	SG + CG	SG + CG
0.5	SG + ISG	SG + ISG	SG + CG
1.0	SG + ISG	SG + ISG	SG + ISG

IG : type D flake graphite RG : type B flake graphite
 SG : spheroidal graphite CG : C/V graphite
 ISG : spheroidal graphite, imperfectly formed

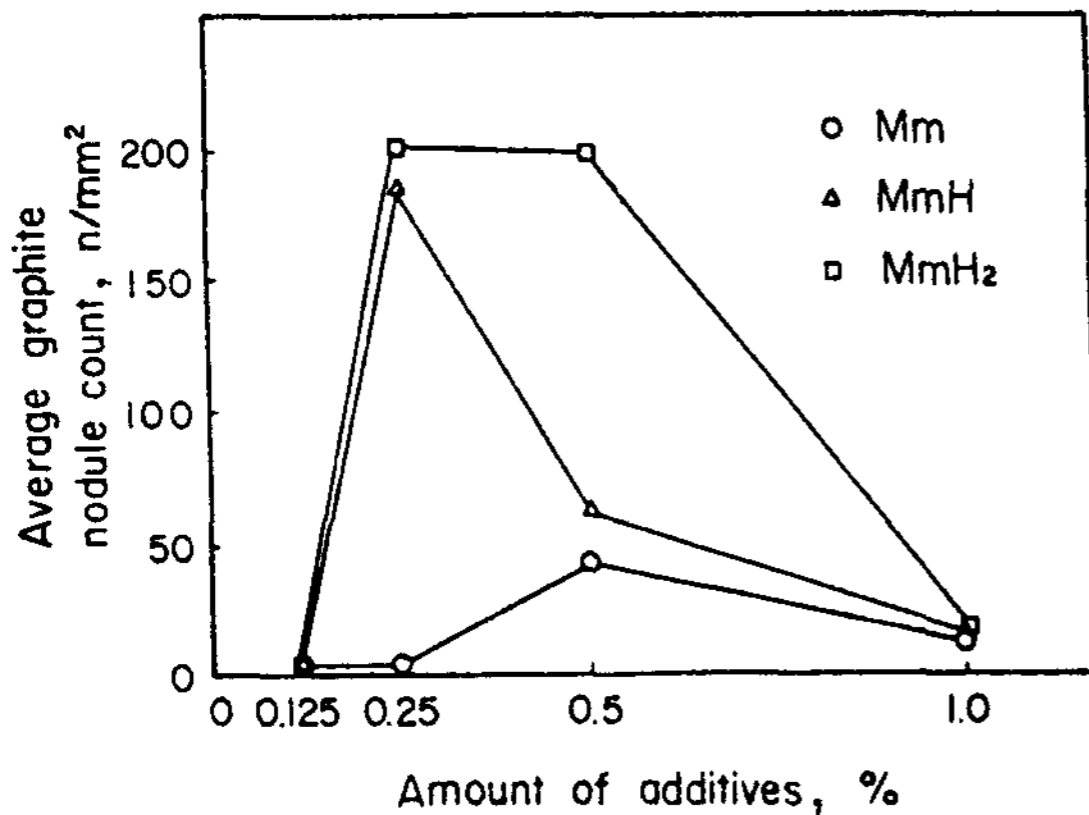


Fig. 6. Variation of the average graphite nodule count with the amount of additives.

big, the value of ΔT_E was as small as 2 to 7 degrees. The spheroidal graphites were formed at the early stage of the eutectic reaction and this structure extended until the end of the eutectic reaction. In this case, the graphite nodule counts were relatively low at 16 to 59n / mm². Since the experimental conditions such as the initial composition of the melt, the melting temperature, the atmosphere, the post inoculation and the cooling rate, except of the nodulizers, were nearly same for all the samples, the difference in the graphite shapes would appear to arise from the differences in the nodulizers, i.e the amount of misch metals and their hydrogen contents. Effects of the rare-earth elements on graphite spheroidization have been investigated by many research-

chers(1,14-16) and it has been found that Ce, Y and La could produce the spheroidal graphites when proper amounts of them were added. Too large an amount of additive, however, would inhibit the graphite spheroidization because the excess of the rare-earth elements formed stable compounds with the other alloying elements in the cast iron and this resulted in a stabilization of the ledeburite. This agreed quite well with our experimental results with the Mm treated samples. That is, addition of less than 0.5%Mm could not produce spheroidal graphite and a greater addition than this produced the spheroidal graphites, but the nodule count decreased with increasing the amount of Mm added. Similar effects of Mm were obtained with the MmH and the MmH₂ treated samples, whereas the hydrogen gave another effect. The role of hydrogen bubbles for production of the spheroidal graphites in cast irons has been examined by Chang et.al. (4,5). They have found that the rare-earth elements (Ce,Y) which were hydrogenated at high temperatures could produce higher nodule counts than those without hydrogenation. However, they did not mention about hydrogen content. From our experimental results it was also shown that MmH and MmH₂ nodulizers caused a drastic increase in the nodule count and in the 0.5%MmH₂ treated sample a significant retardation of the ledeburite formation was observed. This could confirm the role of hydrogen bubbles for the production of spheroidal graphites. The retardation of the ledeburite formation might have resulted from the increase of spheroidal graphites by the increase of hydrogen bubbles. Now it should be discussed a quantitative relationship between the hydrogen bubbles and the misch metal content in the melt in regard with graphite spheroidization. Our experimental results imply that graphite spheroidization is achieved mostly due to the presence of hydrogen bubbles which are introduced by Mm, MmH or MmH₂ addition and become the nucleation sites for the spheroidization. The rare-earth elements in Mm, MmH and MmH₂ should act as ledeburite stabilizers and thus inhibit the graphite spheroidization. These competitive behaviors would depend strongly on absolute and relative amounts of hydrogen and misch metal. When the absolute amounts of hydrogen and misch metal are too small, mixture of the undercooled graphite and

rosette graphite will be obtained. Each sample of the 0.125 %Mm, 0.25 %Mm, 0.125 %MmH and 0.125 %MmH₂ treated are of this case. If sufficient hydrogen bubbles are provided and misch metal is low, high counts of spheroidal and CV graphites are formed. The 0.25 %MmH, 0.25 %MmH₂ and 0.5 %MmH₂ treated samples can be categorized to this type. In the case of 0.5 %MmH₂ treated sample, although the absolute amount of misch-metal might be enough to form ledeburite, the amount of hydrogen bubbles would be relatively greater than misch metal. It should be noted that when the amount of hydrogen added with Mm increases, it will decrease the ratio of the effective hydrogen to produce spheroidal graphite to the total amount of hydrogen added. This is reasonable because the more the hydrogen is added the more the hydrogen bubbles of large size occur, and by the Stoke's law the large hydrogen bubbles can float out quickly from the melt. The misch metal, however, will not be evaporated to the same extent. In addition to this, the rare-earth elements in the misch metal can reabsorb the hydrogen during the cooling. Thus, when large amounts of hydrogen and misch metal are added the effect of hydrogen bubbles may be smaller than that of misch metal. This can be applied to the cases of the 0.5 %MmH, 1.0 %MmH and 1.0 %MmH₂ treated samples in which ledeburite structures with relatively low nodule counts were obtained. In the cases of the 0.5 %Mm, 1.0 %Mm treated samples the absolute amounts of hydrogen were small while the amounts of misch metals were large.

4. Conclusions

In this study we have investigated the effects of Mm, MmH and MmH₂ on production of the spheroidal graphites. The conclusive summary is as follows:

- 1) Spheroidal and/or CV graphites were obtained when more than 0.5 %Mm, 0.25 %MmH or 0.25 %MmH₂ was used as a nodulizer.
- 2) The misch metal hydrides produced much higher nodule counts than the misch metal did and this would be due to the larger amount of hydrogen bubbles introduced by the misch metal hydrides.
- 3) When large amounts of the misch metal or the

misch metal hydrides were added, the nodule counts decreased and ledeburites were formed. This could be attributed to the relatively larger amount of misch metal than the hydrogen bubbles due to the low recovery ratio of hydrogen and the hydrogen reabsorption by the misch metal.

- 4) The bubble theory as one of the graphite spheroidization mechanisms was confirmed.

Reference.

1. A.F.Spengler and H.K.Briggs : "The Ductile Iron Process", Vol.1, Miller & Co., Chicago(1972), 113
2. J.M.Dong, W.A.Henning and J.R.Ward : AFS Transactions, 86(1978),163
3. B.Chang, K.A.Kechi and K. Hanawa: "The spheroidal Graphite Cast Iron", Vol.1, Agne, Tokyo(1983), 54,56
4. B.Chandg, S.Yamamoto, Y.Kawano and R.Ozaki: J.of the Japan Inst.of Metals, 41(1977), 464
5. B.Chandg, S.Yamamoto, Y.Kawano and R.Ozaki: J.of the Japan Inst.of Metals, 41(1977), 471
6. B.Chandg, S.Yamamoto, Y.Kawano and R.Ozaki: J.of the Japan Inst.of Metals, 41(1977), 479
7. B.Chandg, S.Yamamoto, Y.Kawano and R.Ozaki: J.of the Japan Inst.of Metals, 41(1977), 1019
8. B.Chandg, S.Yamamoto, Y.Kawano and R.Ozaki: J.of the Japan Foundrymen's Soc., 49(1977),269
9. B.Chandg, S.Yamamoto, Y.Kawano and R.Ozaki: J.of the Japan Inst.of Metals, 41(1977), 564
10. B.Chandg, S.Yamamoto, Y.Kawano and R.Ozaki: J.of the Japan Inst.of Metals, 41(1977), 571
11. K.Suzuki, S.Q. Guo and M.Imabayashi: J.of the Japan Foundrymen's Soc., 57(1985),232
12. N.Tsutsui and M.Lmamura: Trans. of the Casting Research Lab.,33(1978),73
13. H.Horie, T.Kowata, K.Abe and A.Chida: J.of the Japan Foundrymen's Soc.,57(1985).778
14. V.M.Popov: Liteinoe Proizvodstvo, No.9(1974), 18
15. Y.Kawano, S.Yamamoto and K.Kurai: J.of the Japan Foundrymen's Soc.,47(1975),394
16. K.A.Didenko, A.P.Lyubchenko, S.P.Sakharov, G.P. Umanskii and Yu.S.Uritskii: Liteinoe Proizvodstvo, No. 8(1975),5